

# Evidence that a 'dynamic knockout' in *Escherichia coli* dihydrofolate reductase does not affect the chemical step of catalysis

E. Joel Loveridge, Enas M. Behiry, Jiannan Guo and Rudolf K. Allemann\*

**The question of whether protein motions play a role in the chemical step of enzymatic catalysis has generated much controversy in recent years. Debate has recently reignited over possible dynamic contributions to catalysis in dihydrofolate reductase, following conflicting conclusions from studies of the N23PP/S148A variant of the *Escherichia coli* enzyme. By investigating the temperature dependence of kinetic isotope effects, we present evidence that the reduction in the hydride transfer rate constants in this variant is not a direct result of impairment of conformational fluctuations. Instead, the conformational state of the enzyme immediately before hydride transfer, which determines the electrostatic environment of the active site, affects the rate constant for the reaction. Although protein motions are clearly important for binding and release of substrates and products, there appears to be no detectable dynamic coupling of protein motions to the hydride transfer step itself.**

One of the most contentious topics in modern enzymology is the potential role of protein motions in the chemical step of enzymatic catalysis. Although ligand association and dissociation steps are known to be accompanied by sometimes very large conformational changes, the coupling of protein dynamics to the chemical coordinate of the reaction is less well defined and is often inferred from indirect evidence such as the temperature dependence of the primary hydrogen kinetic isotope effects (KIEs) on the reaction<sup>1–3</sup>, or by computational methods<sup>4–7</sup>.

Hydrogen (as hydride, hydrogen radical or proton) transfer reactions are often used to investigate the potential involvement of protein motions in driving the chemistry of enzyme-catalysed reactions. In these reactions, quantum-mechanical tunnelling plays a role, and the width of the reaction barrier is as important in determining the reaction rate as its height. That hydrogen tunnels in enzymatic reactions may be unsurprising given its small mass, but recognition of hydrogen tunnelling has led to proposals that enzymes may have evolved to enhance the degree of tunnelling so as to accelerate the reaction, and that enzyme dynamics may couple to the reaction coordinate to promote tunnelling both by optimising the wavefunction overlap between the reactant and product states and by decreasing the donor–acceptor distance<sup>1,2,8,9</sup>. These protein motions may range from microsecond to millisecond conformational fluctuations to localized subnanosecond 'promoting vibrations'<sup>1,10–13</sup>. Although both experimental<sup>14,15</sup> and computational studies<sup>16</sup> suggest that the degree of tunnelling is not increased in enzymatic reactions relative to the equivalent reactions in solution, and therefore that the contribution from tunnelling to catalysis is negligible, whether or not protein motions promote hydrogen transfer is less clear and remains an issue of debate<sup>1,2,10,17</sup>.

Although current models that relate a potential role of protein motions in promoting hydrogen transfer to the temperature dependence of the KIE are not consistent with all available data<sup>1,2,16–18</sup>, it is clear that the KIE is highly sensitive to changes in the donor–acceptor distance and the degree of wavefunction overlap between the reactant and product states (affected by both

donor–acceptor distance and the angle of approach, and similar to the more classical concept of orbital overlap)<sup>1,2,8,19,20</sup>. Hence, if conformational fluctuations are directly linked to the chemical step of the reaction cycle and therefore affect either of these parameters, then they will play a role in determining the KIE on hydride transfer. Perturbation of these conformational fluctuations will therefore have an effect on the KIEs. However, it is not sufficient to measure the KIE at a single temperature, as equilibrium changes to the enzyme structure may counteract any potential changes brought about by alteration of the dynamics. The temperature dependence of the KIE is therefore a highly sensitive and much used<sup>1–3,21–28</sup> probe of the changes to the reaction, as it is unlikely that conflicting factors will exactly counterbalance over a wider temperature range.

The potential role of motions in promoting the chemical step of the reaction has been extensively studied in dihydrofolate reductase (DHFR). EcDHFR, the enzyme from *Escherichia coli*, adopts two major conformations—closed and occluded (Fig. 1)—as it moves through its catalytic cycle<sup>29</sup>. These conformations take their names from the position of the M20 loop (residues 9–24), which forms part of the active site. Before the chemical step of the cycle, this loop closes over the active site, shielding the reactants from solvent and providing an optimal environment for protonation of N5 of the dihydrofolate and hydride transfer to occur. This closed conformation is stabilized by hydrogen bonding to the neighbouring FG loop (residues 116–132). In the product complexes, however, the FG loop occludes the active site, preventing the nicotinamide ring of the cofactor NADP(H) from entering. This occluded conformation is stabilized by a pair of hydrogen bonds between residue N23 on the M20 loop and S148 on the GH loop (residues 142–149; Fig. 1). The chemical step of the reaction, hydride transfer from NADPH to dihydrofolate with concomitant protonation of dihydrofolate, occurs within the closed conformation<sup>29</sup>.

A 'dynamic knockout' of EcDHFR has recently been reported, in which mutations were made that both prevent formation of the occluded conformation through loss of hydrogen bonding

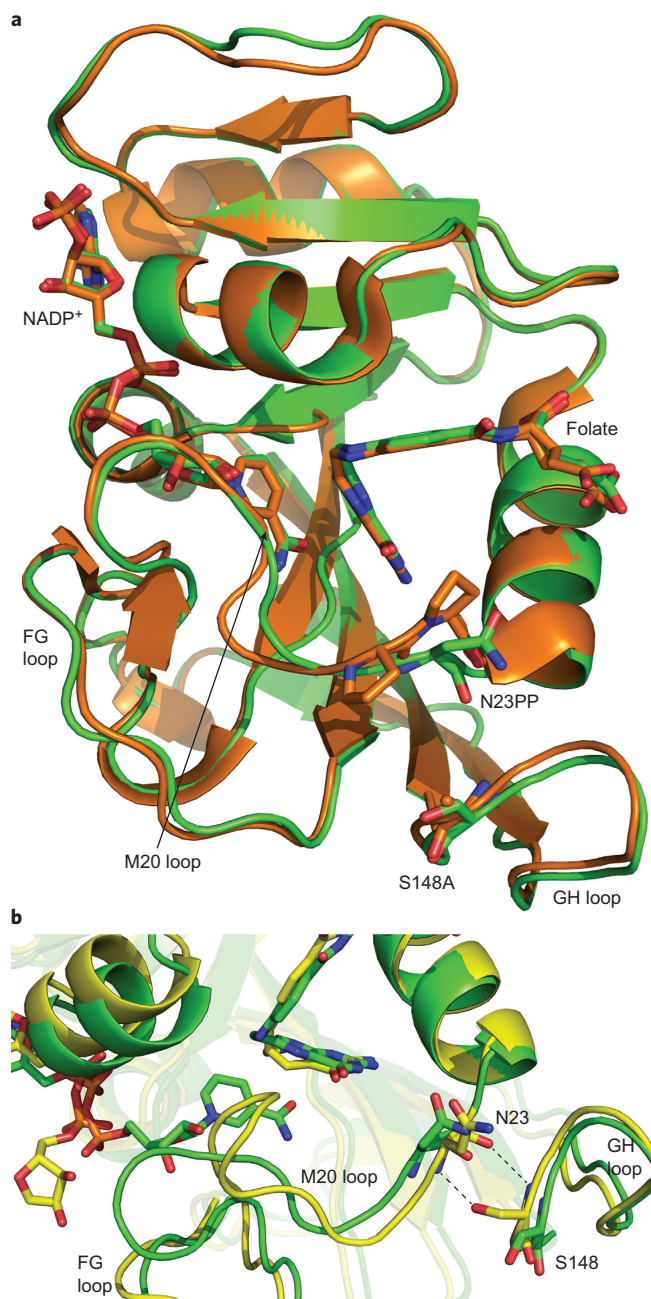


**Figure 1 | Crystal structures of wild-type EcDHFR and EcDHFR-N23PP/S148A.** **a**, Cartoon representations of wild-type EcDHFR (green, PDB 1RX2<sup>29</sup>) and EcDHFR-N23PP/S148A (orange, PDB 3QL0<sup>30</sup>) as DHFR:NADP<sup>+</sup>:folate complexes, which serve as a model for the DHFR:NADPH: dihydrofolate Michaelis complexes<sup>29</sup>. Note the high similarity in the overall fold of the two enzymes. **b**, Detailed view of the catalytically important M20 loop in the closed (green, PDB 1RX2<sup>29</sup>) and occluded (yellow, PDB 1RX4<sup>29</sup>) conformations in EcDHFR. In the closed conformation, the substrate dihydrofolate and the cofactor NADPH are positioned ready for hydride transfer to occur and the M20 loop shields the active site from solvent. In the occluded conformation, the M20 loop prevents access of the nicotinamide ring of NADP(H) to the active site. Ligands and amino acids replaced in the EcDHFR variant are shown as sticks. Structural elements discussed in the text and hydrogen bonding between the M20 and GH loops in the occluded conformation are indicated.

between the M20 and GH loops (Fig. 1) and eliminate millisecond to timescale motions of the M20 loop in the Michaelis complex<sup>30</sup>. This EcDHFR-N23PP/S148A variant displayed a reduced rate

constant for hydride transfer and it was suggested that this was a consequence of the loss of conformational flexibility<sup>30</sup>. However, a subsequent computational study suggested instead that the reduced rate constant is a consequence of changes to the reorganization free energy of the reaction brought about by changes to the electrostatic preorganization within the active site<sup>31</sup>. Here, we investigate the effect of the N23PP/S148A mutations on EcDHFR catalysis, and provide experimental evidence that the nature of the chemistry in this ‘dynamic knockout’ of EcDHFR is essentially the same as in the wild-type enzyme.

## Results and discussion

### Creation of EcDHFR-N23PP/S148A and structural studies.

EcDHFR-N23PP/S148A was created using standard site-directed mutagenesis techniques. The purified protein was first characterized by circular dichroism spectroscopy, which showed only minor differences to the wild-type enzyme (Supplementary Fig. S1). It has previously been shown that the NADP<sup>+</sup>:folate complex of EcDHFR-N23PP/S148A has a similar structure to that of the wild-type enzyme<sup>30</sup>. The melting temperature of EcDHFR-N23PP/S148A was found to be  $56.8 \pm 0.2$  °C, which is slightly higher than the value of  $51.6 \pm 0.7$  °C obtained for the wild-type enzyme<sup>32</sup>, suggesting that the N23PP and S148A mutations have a stabilizing effect on the enzyme.

**Steady-state kinetics.** Michaelis–Menten curves for both substrate and cofactor were measured at 20 °C and pH 7. The Michaelis constants were found to be  $2.4 \pm 0.3$   $\mu$ M for NADPH and  $0.7 \pm 0.2$   $\mu$ M for dihydrofolate. These are in good agreement with the values of  $4.8 \pm 1.0$   $\mu$ M and  $0.7 \pm 0.2$   $\mu$ M obtained at 25 °C for wild-type EcDHFR<sup>33</sup>, demonstrating that the affinity of the enzyme for its reactants is not significantly affected by the N23PP/S148A mutations. The value of  $k_{\text{cat}}$  was found to be  $1.94 \pm 0.09$  s<sup>−1</sup> at 20 °C, in good agreement with the reported value<sup>30</sup>. The temperature dependence of  $k_{\text{cat}}$  was determined at pH 7 (Supplementary Table S1). The activation energy was found to be  $52.6 \pm 1.2$  kJ mol<sup>−1</sup>, which is only slightly higher than that of the wild-type enzyme ( $47.7 \pm 0.8$  kJ mol<sup>−1</sup>)<sup>34</sup>, as expected from the relatively small (~sixfold) reduction in  $k_{\text{cat}}$ . It should be noted, however, that direct comparison of the activation energies is mechanistically uninformative as a different step within the catalytic cycle is rate limiting in EcDHFR-N23PP/S148A than in the wild-type enzyme<sup>30</sup>. The primary hydrogen KIE on  $k_{\text{cat}}$  was only slightly higher than unity at pH 7 ( $1.49 \pm 0.07$ ), but was  $2.79 \pm 0.02$  at pH 9. This is in agreement with the steady-state rate constant being predominantly limited by a physical step of the catalytic cycle at pH 7 (with some contribution from the chemical step, as expected from the relatively low hydride transfer rates<sup>30</sup>), but almost exclusively limited by the chemical step at elevated pH, as had been seen for wild-type EcDHFR<sup>33</sup>.

**Single turnover kinetics.** The  $k_{\text{cat}}$  at pH 7 is dominated by physical steps within the reaction cycle (*vide supra*), so its KIE cannot be interpreted mechanistically. Therefore, to investigate the effect of the ‘dynamic knockout’<sup>30</sup> on the chemical step of EcDHFR catalysis, the temperature dependence of the KIE on the hydride transfer step of catalysis, isolated under single turnover stopped-flow conditions, was determined at pH 7 and 9 (Fig. 2, Table 1 and Supplementary Tables S2–S5). It has been shown recently that the KIE on hydride transfer in EcDHFR is temperature-dependent below pH 8 and temperature-independent at or above this pH, demonstrating that the temperature-dependent KIEs observed at pH 7 are indeed physiologically relevant, and the temperature-independent KIEs observed at elevated pH, where hydride transfer is rate-limiting<sup>33</sup>, are not<sup>21</sup>.

The rate constants for hydride ( $k_{\text{H}}$ ) and deuteride ( $k_{\text{D}}$ ) transfer were considerably lower than those of the wild-type enzyme

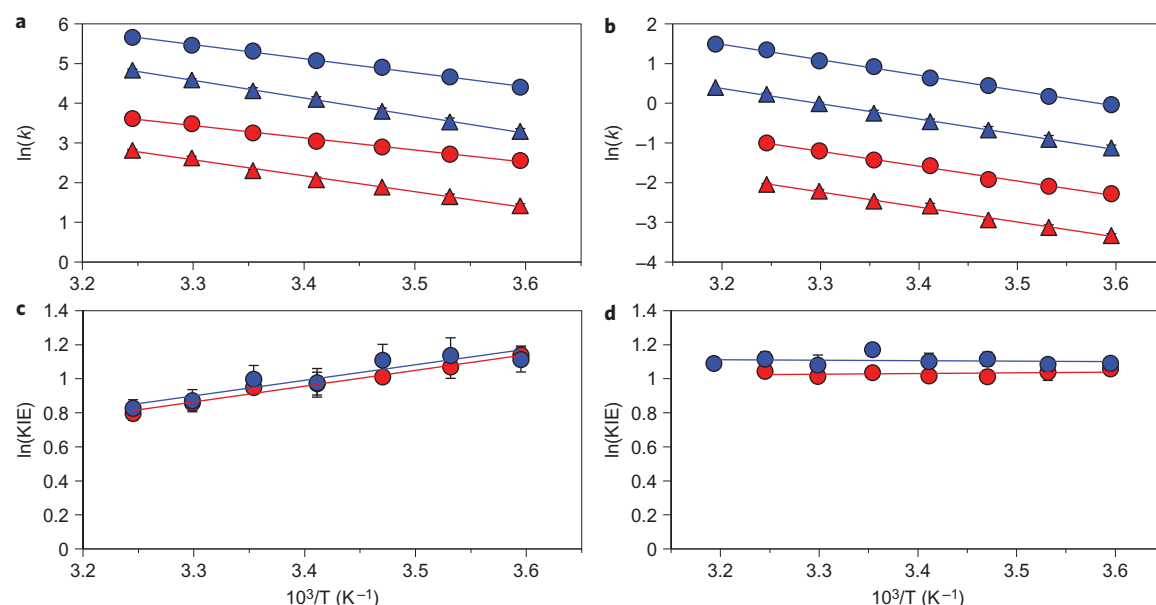


**Figure 2 | Pre-steady-state kinetics of EcDHFR and EcDHFR-N23PP/S148A.** **a**, Arrhenius plots for hydride (circles) and deuteride (triangles) transfer for EcDHFR (blue) and EcDHFR-N23PP/S148A (red) at pH 7. **b**, Arrhenius plots for hydride (circles) and deuteride (triangles) transfer for wild-type EcDHFR (blue) and EcDHFR-N23PP/S148A (red) at pH 9. **c**, Plots of KIE on a logarithmic abscissa against the inverse temperature for wild-type EcDHFR (blue) and EcDHFR-N23PP/S148A (red) at pH 7. **d**, Plots of KIE on a logarithmic abscissa against inverse temperature for wild-type EcDHFR (blue) and EcDHFR-N23PP/S148A (red) at pH 9. Error bars (standard errors of the mean at  $1\sigma$ ) are small and hence obscured by the symbols in most cases. The data show that, although there are large differences between the rate constants for hydride transfer in EcDHFR and EcDHFR-N23PP/S148A, the magnitude and temperature dependence of the KIE are virtually identical.

(Table 1 and Fig. 2)<sup>30</sup>. Both the magnitude and temperature dependence of the KIE on the reaction catalysed by EcDHFR-N23PP/S148A, on the other hand, were almost indistinguishable from those of wild-type EcDHFR. The values of  $k_H$  obtained here ( $25.9 \pm 0.3 \text{ s}^{-1}$  at pH 7 and  $0.24 \pm 0.01 \text{ s}^{-1}$  at pH 9 at  $25^\circ\text{C}$ ) are slightly different to those published previously (14 and  $3.3 \text{ s}^{-1}$ , respectively<sup>30</sup>). Activation enthalpies were slightly reduced in EcDHFR-N23PP/S148A, with the activation entropy accounting for the higher activation free energy and corresponding lower rate constants. The activation entropy for hydride transfer by EcDHFR-N23PP/S148A is  $\sim 30 \text{ J K}^{-1} \text{ mol}^{-1}$  more negative than that of the wild-type enzyme at pH 7 (Table 1). The potential energy surface is therefore probably flatter in the conformational direction in the wild-type enzyme than in EcDHFR-N23PP/S148A, as has been found recently in a computational study<sup>31</sup>. The values of  $\Delta G^\ddagger$  obtained here (Table 1) are in excellent agreement with recently calculated values<sup>31</sup>. We also note that the similarity of the magnitude of the KIE for EcDHFR-N23PP/S148A and EcDHFR suggests that the two enzymes have indistinguishable donor–acceptor distances in the Michaelis complexes, in contrast to what was observed in the X-ray crystal structures of the E:NADP<sup>+</sup>:folate complexes, where this distance was reported to differ by  $0.3 \text{ \AA}$  (ref. 30). We have previously shown that changes to the donor–acceptor distance as small as  $0.05 \text{ \AA}$  are detectable using our methodology<sup>35</sup>.

It has been suggested that the lower hydride transfer rate constants in EcDHFR-N23PP/S148A relative to the wild-type enzyme are the result of the loss of conformational flexibility in the variant enzyme<sup>30</sup>. Although Bhabha *et al.* state that ‘the decreased hydride transfer rate does not simply arise from impairment of the closed-to-occluded transition’<sup>30</sup>, they argue that as EcDHFR-S148A, unlike EcDHFR-N23PP/S148A, retains millisecond conformational fluctuations in regions of the active site other than the M20 loop, and has only a slightly lower rate constant for hydride transfer than wild-type EcDHFR, millisecond

conformational motions other than the closed-to-occluded conformational change ‘probably play a role in hydride transfer’<sup>30</sup>. The occluded conformation itself cannot be relevant to the chemical step of the catalytic cycle because the nicotinamide ring of NADP(H) is not within the active site and so cannot react<sup>29</sup>. In addition, for the M20 loop to move from the closed to the occluded conformation, the loop must first open to allow the nicotinamide ring to leave the active site<sup>29,36</sup>. We have already provided evidence that fluctuations between the excited-state closed conformation and the ground-state occluded conformation seen by NMR in the EcDHFR:NADP<sup>+</sup>:tetrahydrofolate product ternary complex are not relevant to the hydride transfer step itself<sup>21</sup>. Similarly, fluctuations between the excited-state occluded conformation and the ground-state closed conformation seen by NMR in the EcDHFR:NADP<sup>+</sup>:folate complex (a model for the Michaelis complex<sup>29</sup>) are not relevant to hydride transfer but are thought to precede it<sup>37</sup>.

Unlike the closed-to-occluded conformational change, other millisecond motions within the active site are not necessarily orthogonal to the reaction coordinate and may therefore affect the reaction chemistry<sup>30</sup>. However, the correlation between the loss of conformational fluctuations and the reduction in the rate constant for hydride transfer seen in EcDHFR-N23PP/S148A does not necessarily demonstrate causation. On the contrary, the similarity between the temperature dependence of the KIEs of the wild-type and variant enzymes strongly suggests that the nature of the chemistry is unaffected by the ‘dynamic knockout’<sup>30</sup> induced by the N23PP/S148A mutations and therefore that the loss of conformational fluctuations is not the cause of the lower hydride transfer rate constants. The KIE is highly sensitive to changes in the donor–acceptor distance. Indeed, changes to the donor–acceptor distance at a fixed temperature cause larger changes to the KIE than temperature does at a fixed donor–acceptor distance<sup>19</sup>. Increasing the donor–acceptor distance increases the temperature dependence of the KIE as well as altering its magnitude<sup>19</sup>, and the



**Table 1 | Kinetic parameters for EcDHFR and EcDHFR-N23PP/S148A at 25 °C.**

Parameter	Wild-type EcDHFR <sup>21</sup>		EcDHFR-N23PP/S148A	
	pH 7	pH 9	pH 7	pH 9
$k_H$ (s <sup>-1</sup> )	203.7 ± 7.4	2.52 ± 0.02	25.9 ± 0.3	0.24 ± 0.01
KIE	2.71 ± 0.08	3.23 ± 0.05	2.58 ± 0.03	2.82 ± 0.06
$E_a^H$ (kJ mol <sup>-1</sup> )	29.9 ± 0.6	32.0 ± 0.6	25.7 ± 0.9	31.1 ± 1.2
$E_a^D$ (kJ mol <sup>-1</sup> )	37.8 ± 0.6	32.0 ± 0.5	33.4 ± 1.2	31.4 ± 1.2
$\Delta E_a$ (kJ mol <sup>-1</sup> )	7.9 ± 0.9	-0.1 ± 0.8	7.7 ± 1.5	0.4 ± 1.7
$A_H$ (s <sup>-1</sup> )	(3.4 ± 0.5) × 10 <sup>7</sup>	(1.0 ± 0.3) × 10 <sup>6</sup>	(8.2 ± 0.2) × 10 <sup>5</sup>	(6.8 ± 0.3) × 10 <sup>4</sup>
$A_D$ (s <sup>-1</sup> )	(3.2 ± 0.1) × 10 <sup>8</sup>	(3.2 ± 0.7) × 10 <sup>5</sup>	(7.4 ± 0.2) × 10 <sup>6</sup>	(2.8 ± 0.1) × 10 <sup>4</sup>
$A_H/A_D$	0.11 ± 0.02	3.08 ± 1.02	0.11 ± 0.04	2.42 ± 0.07
$\Delta H_H^\ddagger$ (kJ mol <sup>-1</sup> )	27.4 ± 0.6	29.6 ± 0.6	23.2 ± 0.9	28.6 ± 1.2
$\Delta H_D^\ddagger$ (kJ mol <sup>-1</sup> )	35.3 ± 0.6	29.5 ± 0.5	30.9 ± 1.2	29.0 ± 1.2
$\Delta S_H^\ddagger$ (J K <sup>-1</sup> mol <sup>-1</sup> )	-109.0 ± 2.5	-138.3 ± 5.1	-139.9 ± 7.5	-160.6 ± 18.4
$\Delta S_D^\ddagger$ (J K <sup>-1</sup> mol <sup>-1</sup> )	-90.3 ± 1.8	-147.7 ± 4.8	-121.6 ± 6.4	-167.9 ± 22.8
$\Delta G_H^\ddagger$ (kJ mol <sup>-1</sup> )	59.9 ± 0.6	70.8 ± 0.6	64.9 ± 0.9	76.5 ± 1.2
$\Delta G_D^\ddagger$ (kJ mol <sup>-1</sup> )	62.2 ± 0.6	73.6 ± 0.5	67.2 ± 1.2	79.1 ± 1.2

effect on the KIE of a change as small as 0.05 Å would be detectable using our methodology<sup>35</sup>. Therefore, if millisecond conformational fluctuations are coupled directly to the chemical step, then it is highly unlikely that changes to these fluctuations would not manifest themselves in either the magnitude or the temperature dependence of the KIE. The only logical conclusion is therefore that no such coupling exists.

We have previously argued against a direct role for conformational and dynamic effects in the chemical step of DHFR catalysis<sup>21,35,38,39</sup>. The data reported here provide further evidence in support of this view. However, the rate constant for the reaction is most probably determined by the conformational state of the enzyme at the point of reaction, because the specific conformation will determine the electrostatics in and around the active site and therefore control the reaction free energy. This conclusion is supported by our observation that the rate constant for hydride transfer (but not the KIE) for the DHFR-catalysed reaction is proportional to the dielectric constant of the medium but not to its viscosity<sup>35,39,40</sup>. Hence, the rate constants for the chemical step appear to be dependent on electrostatic effects but not directly influenced by large-scale dynamical contributions. It is therefore more likely that the dampening of the millisecond motions around the active site brings about more subtle conformational changes. This is not a semantic argument; although our results show that the difference in catalytic properties of EcDHFR and EcDHFR-N23PP/S148A are indeed a simple consequence of electrostatic effects as has been argued previously<sup>31</sup>, these electrostatic effects are affected by the conformational state of the enzyme and its effect on the energy landscape of the reaction. However, this is an equilibrium property of the enzyme and no dynamic contribution from protein motions to the reaction is required.

As well as showing that millisecond dynamics do not directly influence the chemical step of the EcDHFR-catalysed reaction, our work demonstrates a clear need both for better theoretical frameworks that can explain non-classical temperature dependences of KIEs on enzymatic hydride transfer (particularly temperature-independent KIEs<sup>18</sup>) and for direct experimental evidence for (or against) a link between protein motions, ligand motions and the chemistry proper. All current evidence supporting a role for DHFR dynamics in the actual chemical step is indirect and largely based on current models of KIEs that may be inadequate given their numerous inconsistencies with both experimental and computational data<sup>1,19,22,30,41,42</sup>. However, no direct experimental evidence that refutes a role for dynamics in the chemical step has been provided either. Even though dynamic contributions to a

millisecond timescale appear to be unimportant, kinetic studies cannot rule out a role for faster motions. New models and experiments are therefore required before the large amount of apparently contradictory evidence relating to the mechanistic underpinning of DHFR catalysis can be reconciled and fully explained.

## Conclusions

The nature of the chemistry, as reported by the magnitude and temperature dependence of the KIEs on hydride transfer, appears to be unaffected in EcDHFR-N23PP/S148A. This demonstrates that, contrary to a recent report<sup>30</sup>, conformational fluctuations do not seem to be directly involved in the chemical step of the reaction. The electrostatic preorganization within the active site during the reaction is determined by the conformational state of the enzyme at the point of reaction; hence, subtle changes to the (equilibrium) conformational state of the enzyme as a consequence of structural changes brought about by amino acid replacements or changes to the conditions of the reaction will nevertheless affect the rate constants for the reaction. As can be seen from the change in rate-limiting step in the steady state<sup>30</sup>, the dynamic properties of EcDHFR and its mutants clearly affect the conformational motions that are important for the turnover of substrate to product, but no correlation between these conformational motions and the chemical motions that direct hydride transfer have yet been identified for DHFR.

## Methods

**Chemicals.** Dihydrofolate was prepared by dithionite reduction of folate (Sigma)<sup>43</sup>. NADPH and 4-(R)-NADPD were prepared from NADP<sup>+</sup> (Melford) as described previously<sup>21</sup>. EcDHFR and EcDHFR-N23PP/S148A were produced in *E. coli* BL21(DE3) cells containing a pET11c-based plasmid encoding the enzymes and purified by anion exchange chromatography on Q-sepharose resin followed by size exclusion chromatography on a prep-grade Superdex 75 column (GE Healthcare). Oligonucleotide primers were purchased from Eurofins. The concentrations of NADPH/NADPD and H<sub>2</sub>F were determined spectrophotometrically using extinction coefficients of 6,200 cm<sup>-1</sup> M<sup>-1</sup> at 339 nm and 28,000 cm<sup>-1</sup> M<sup>-1</sup> at 282 nm, respectively<sup>42</sup>.

**Site-directed mutagenesis.** A gene encoding EcDHFR-N23PP/S148A was created using the Finnzymes Phusion site directed mutagenesis kit and primers 5'-GAAAACGCCATGCCGTGGCCGCCGCTGCCTGCCGATCTCGCC-3' (N23PP) and 5'-GCGCAGAACGCTCACAGCTATTGC-3' (S148A). The altered and inserted nucleotides are underlined.

**Circular dichroism spectroscopy.** Circular dichroism spectra between 190 and 400 nm were measured in a nitrogen atmosphere by an Applied Photophysics Chirascan spectrophotometer using 12.5 μM protein in 10 mM potassium phosphate buffer (pH 7.0). Mean residue ellipticities [Θ]<sub>MRE</sub> were calculated using the equation [Θ]<sub>MRE</sub> = Θ/(10ncl), where Θ is the measured ellipticity (in mdeg), n the number of backbone amide bonds, c the protein concentration (in mol l<sup>-1</sup>) and l the path length (in cm). Thermal denaturation experiments were performed between

10 and 80 °C using temperature steps of 1 °C with 1 min equilibration at the desired temperature before measurement. Melting temperatures were determined from the change in signal at 222 nm against temperature.

**Steady-state kinetic measurements.** Steady-state turnover rates were determined spectrophotometrically using a JASCO V-660 spectrophotometer by following the decrease in absorbance at 340 nm ( $\epsilon_{340}(\text{NADPH} + \text{H}_2\text{F}) = 11,800 \text{ M}^{-1} \text{ cm}^{-1}$ )<sup>44</sup>. Potassium phosphate (100 mM) containing 100 mM NaCl and 10 mM  $\beta$ -mercaptoethanol was used for measurements at pH 7, and at pH 9, MTEN buffer (50 mM morpholinoethanesulfonic acid, 25 mM Tris, 25 mM ethanolamine, 100 mM NaCl and 10 mM  $\beta$ -mercaptoethanol) was used. Phosphate buffer was used at pH 7 as its  $pK_a$  is relatively insensitive to changes in temperature<sup>45</sup>. The enzyme (50 nM) was pre-incubated at the desired temperature with NADPH (0.5–100  $\mu\text{M}$ ) for 1 min to avoid hysteresis<sup>11</sup> before the addition of  $\text{H}_2\text{F}$  (0.5–100  $\mu\text{M}$ ). For the temperature dependence of  $k_{\text{cat}}$  or for KIE measurements, 100  $\mu\text{M}$  each of both substrate and cofactor were used. The change in initial rate with concentration was fit to the Michaelis–Menten equation using SigmaPlot 10. Each data point is the result of three independent measurements.

**Pre-steady-state kinetic measurements.** The chemical step was observed under single turnover conditions from the loss of fluorescence resonance energy transfer from the enzyme to NADPH during the reaction. The enzyme (20  $\mu\text{M}$  final concentration) was pre-incubated with NADPH (8  $\mu\text{M}$  final concentration) for at least 5 min in 100 mM potassium phosphate buffer (pH 7.0) containing 100 mM NaCl and 10 mM  $\beta$ -mercaptoethanol or MTEN (*vide supra*) buffer (pH 9.0). The reaction was then initiated by rapidly mixing in  $\text{H}_2\text{F}$  (200  $\mu\text{M}$  final concentration) in the same buffer. Varying the concentrations of the reagents showed that the measured rate constants were limiting values. Measurements were made on either an Applied Photophysics stopped-flow spectrophotometer, exciting the sample at 292 nm and measuring the emission using a 400 nm cutoff output filter, or a Hi-Tech Scientific stopped-flow spectrophotometer, exciting the sample at 297 nm and measuring the emission above 440 nm. Identical results were obtained with both set-ups. All experiments were repeated at least three times on each spectrometer.

Received 18 November 2011; accepted 6 February 2012;  
published online 11 March 2012

## References

- Nagel, Z. D. & Klinman, J. P. A 21st century revisionist's view at a turning point in enzymology. *Nature Chem. Biol.* **5**, 543–550 (2009).
- Limbach, H.-H., Schowen, K. B. & Schowen, R. L. Heavy atom motions and tunneling in hydrogen transfer reactions: the importance of the pre-tunneling state. *J. Phys. Org. Chem.* **23**, 586–605 (2010).
- Allemann, R. K., Evans, R. M. & Loveridge, E. J. Probing coupled motions in enzymatic hydrogen tunnelling reactions. *Biochem. Soc. Trans.* **37**, 349–353 (2009).
- Masgrau, L. *et al.* Atomic description of an enzyme reaction dominated by proton tunneling. *Science* **312**, 237–241 (2006).
- Antonioni, D., Basner, J., Núñez, S. & Schwartz, S. D. Computational and theoretical methods to explore the relation between enzyme dynamics and catalysis. *Chem. Rev.* **106**, 3170–3187 (2006).
- Olsson, M. H. M., Parson, W. W. & Warshel, A. Dynamical contributions to enzyme catalysis: critical tests of a popular hypothesis. *Chem. Rev.* **106**, 1737–1756 (2006).
- McGeagh, J. D., Ranaghan, K. E. & Mulholland, A. J. Protein dynamics and enzyme catalysis: insights from simulations. *Biochim. Biophys. Acta* **1814**, 1077–1092 (2011).
- Kuznetsov, A. & Ulstrup, J. Proton and hydrogen atom tunnelling in hydrolytic and redox enzyme catalysis. *Can. J. Chem.* **77**, 1085–1096 (1999).
- Sutcliffe, M. J. & Scrutton, N. S. Enzymology takes a quantum leap forward. *Phil. Trans. R. Soc. Lond. A* **358**, 367–386 (2000).
- Pudney, C. R. *et al.* Evidence to support the hypothesis that promoting vibrations enhance the rate of an enzyme catalyzed H-tunneling reaction. *J. Am. Chem. Soc.* **131**, 17072–17073 (2009).
- Schwartz, S. D. & Schramm, V. L. Enzymatic transition states and dynamic motion in barrier crossing. *Nature Chem. Biol.* **5**, 551–558 (2009).
- Pineda, J. R. E. T., Antonioni, D. & Schwartz, S. D. Slow conformational motions that favor sub-picosecond motions important for catalysis. *J. Phys. Chem. B* **114**, 15985–15990 (2010).
- Henzler-Wildman, K. & Kern, D. Dynamic personalities of proteins. *Nature* **450**, 964–972 (2007).
- Doll, K. M. & Finke, R. G. A compelling experimental test of the hypothesis that enzymes have evolved to enhance quantum mechanical tunneling in hydrogen transfer reactions: the beta-neopentylcobalamin system combined with prior adocobalamin data. *Inorg. Chem.* **42**, 4849–4856 (2003).
- Doll, K. M., Bender, B. R. & Finke, R. G. The first experimental test of the hypothesis that enzymes have evolved to enhance hydrogen tunneling. *J. Am. Chem. Soc.* **125**, 10877–10884 (2003).
- Kamerlin, S. C. L. & Warshel, A. An analysis of all the relevant facts and arguments indicates that enzyme catalysis does not involve large contributions from nuclear tunneling. *J. Phys. Org. Chem.* **23**, 677–684 (2010).
- Pisliakov, A. V., Cao, J., Kamerlin, S. C. L. & Warshel, A. Enzyme millisecond conformational dynamics do not catalyze the chemical step. *Proc. Natl Acad. Sci. USA* **106**, 17359–17364 (2009).
- Romesberg, F. E. & Schowen, R. L. Isotope effects and quantum tunneling in enzyme-catalyzed hydrogen transfer. Part I. The experimental basis. *Adv. Phys. Org. Chem.* **39**, 27–77 (2004).
- Liu, H. & Warshel, A. Origin of the temperature dependence of isotope effects in enzymatic reactions: the case of dihydrofolate reductase. *J. Phys. Chem. B* **111**, 7852–7861 (2007).
- Wu, Y. D. & Houk, K. Theoretical transition structures for hydride transfer to methyleniminium ion from methylamine and dihydropyridine. On the nonlinearity of hydride transfers. *J. Am. Chem. Soc.* **109**, 2226–2227 (1987).
- Loveridge, E. J. & Allemann, R. K. Effect of pH on hydride transfer by *Escherichia coli* dihydrofolate reductase. *ChemBioChem* **12**, 1258–1262 (2011).
- Sikorski, R. S. *et al.* Tunneling and coupled motion in the *Escherichia coli* dihydrofolate reductase catalysis. *J. Am. Chem. Soc.* **126**, 4778–4779 (2004).
- Kohen, A., Cannio, R., Bartolucci, S. & Klinman, J. P. Enzyme dynamics and hydrogen tunnelling in a thermophilic alcohol dehydrogenase. *Nature* **399**, 496–499 (1999).
- Chowdhury, S. & Banerjee, R. Evidence for quantum mechanical tunneling in the coupled cobalt–carbon bond homolysis–substrate radical generation reaction catalyzed by methylmalonyl-CoA mutase. *J. Am. Chem. Soc.* **122**, 5417–5418 (2000).
- Fan, F. & Gadda, G. Oxygen- and temperature-dependent kinetic isotope effects in choline oxidase: correlating reversible hydride transfer with environmentally enhanced tunneling. *J. Am. Chem. Soc.* **127**, 17954–17961 (2005).
- Anandarajah, K. & Schowen, K. Hydrogen tunneling in glucose oxidation by the archaeon *Thermoplasma acidophilum*. *Z. Phys. Chem.* **222**, 1333–1347 (2008).
- Hay, S., Pudney, C. R. & Scrutton, N. S. Structural and mechanistic aspects of flavoproteins: probes of hydrogen tunnelling. *FEBS J.* **276**, 3930–3941 (2009).
- Heyes, D. J., Sakuma, M., de Visser, S. P. & Scrutton, N. S. Nuclear quantum tunneling in the light-activated enzyme protochlorophyllide oxidoreductase. *J. Biol. Chem.* **284**, 3762–3767 (2009).
- Sawaya, M. R. & Kraut, J. Loop and subdomain movements in the mechanism of *Escherichia coli* dihydrofolate reductase: crystallographic evidence. *Biochemistry* **36**, 586–603 (1997).
- Bhabha, G. *et al.* A dynamic knockout reveals that conformational fluctuations influence the chemical step of enzyme catalysis. *Science* **332**, 234–238 (2011).
- Adamczyk, A. J., Cao, J., Kamerlin, S. C. L. & Warshel, A. Catalysis by dihydrofolate reductase and other enzymes arises from electrostatic preorganization, not conformational motions. *Proc. Natl Acad. Sci. USA* **108**, 14115–14120 (2011).
- Swanwick, R. S., Shrimpton, P. J. & Allemann, R. K. Pivotal role of Gly 121 in dihydrofolate reductase from *Escherichia coli*: the altered structure of a mutant enzyme may form the basis of its diminished catalytic performance. *Biochemistry* **43**, 4119–4127 (2004).
- Fierke, C. A., Johnson, K. A. & Benkovic, S. J. Construction and evaluation of the kinetic scheme associated with dihydrofolate reductase from *Escherichia coli*. *Biochemistry* **26**, 4085–4092 (1987).
- Maglia, G., Javed, M. H. & Allemann, R. K. Hydride transfer during catalysis by dihydrofolate reductase from *Thermotoga maritima*. *Biochem. J.* **374**, 529–535 (2003).
- Loveridge, E. J. *et al.* The role of large-scale motions in catalysis by dihydrofolate reductase. *J. Am. Chem. Soc.* **133**, 20561–20570 (2011).
- Arora, K. & Brooks, C. L. III Functionally important conformations of the Met20 loop in dihydrofolate reductase are populated by rapid thermal fluctuations. *J. Am. Chem. Soc.* **131**, 5642–5647 (2009).
- Osborne, M. J., Schnell, J., Benkovic, S. J., Dyson, H. J. & Wright, P. E. Backbone dynamics in dihydrofolate reductase complexes: role of loop flexibility in the catalytic mechanism. *Biochemistry* **40**, 9846–9859 (2001).
- Loveridge, E. J. & Allemann, R. K. The temperature dependence of the kinetic isotope effects of dihydrofolate reductase from *Thermotoga maritima* is influenced by intersubunit interactions. *Biochemistry* **49**, 5390–5396 (2010).
- Loveridge, E. J., Tey, L.-H. & Allemann, R. K. Solvent effects on catalysis by *Escherichia coli* dihydrofolate reductase. *J. Am. Chem. Soc.* **132**, 1137–1143 (2010).
- Loveridge, E. J., Evans, R. M. & Allemann, R. K. Solvent effects on environmentally coupled hydrogen tunnelling during catalysis by dihydrofolate reductase from *Thermotoga maritima*. *Chem. Eur. J.* **14**, 10782–10788 (2008).

41. Liu, H. & Warshel, A. The catalytic effect of dihydrofolate reductase and its mutants is determined by reorganization energies. *Biochemistry* **46**, 6011–6025 (2007).
42. Swanwick, R. S., Maglia, G., Tey, L.-H. & Allemann, R. K. Coupling of protein motions and hydrogen transfer during catalysis by *Escherichia coli* dihydrofolate reductase. *Biochem. J.* **394**, 259–265 (2006).
43. Blakley, R. Crystalline dihydropteroylglutamic acid. *Nature* **188**, 231–232 (1960).
44. Stone, S. R. & Morrison, J. F. Kinetic mechanism of the reaction catalyzed by dihydrofolate reductase from *Escherichia coli*. *Biochemistry* **21**, 3757–3765 (1982).
45. Reijenga, J. C., Gagliardi, L. G. & Kenndler, E. Temperature dependence of acidity constants, a tool to affect separation selectivity in capillary electrophoresis. *J. Chromatogr. A* **1155**, 142–145 (2007).

## Acknowledgements

This work was supported by the UK Biotechnology and Biological Sciences Research Council (BBSRC) (grant no. BB/E008380/1) and by Cardiff University.

## Author contributions

E.J.L. performed the bulk of the experimental work. E.M.B. and J.G. performed additional experiments. E.J.L. and R.K.A. designed the experiments, analysed the data and wrote the manuscript. All authors commented on the manuscript.

## Additional information

The authors declare no competing financial interests. Supplementary information accompanies this paper at [www.nature.com/naturechemistry](http://www.nature.com/naturechemistry). Reprints and permission information is available online at <http://www.nature.com/reprints>. Correspondence and requests for materials should be addressed to R.K.A.